Multiple causes of interannual sea surface temperature variability in the equatorial Atlantic Ocean

INGO RICHTER, SWADHIN K. BEHERA

Research Institute for Global Change, JAMSTEC, Yokohama, Japan, and Application Laboratory, JAMSTEC, Yokohama, Japan

YUKIO MASUMOTO

Research Institute for Global Change, JAMSTEC, Yokohama, Japan

BUNMEI TAGUCHI, HIDEHARU SASAKI

Earth Simulator Center, JAMSTEC, Yokohama, Japan

TOSHIO YAMAGATA

Department of Earth and Planetary Sciences, University of Tokyo, Tokyo, Japan, and Application Laboratory, JAMSTEC, Yokohama, Japan

Nature Geoscience

27 September 2012, submitted

7 November 2012, revised

9 November 2012, accepted

Corresponding author:

Ingo Richter

Research Institute for Global Change, JAMSTEC, Yokohama, Japan

E-mail: richter@jamstec.go.jp

The eastern equatorial Atlantic Ocean is subject to interannual fluctuations of sea surface temperatures, with climatic impacts on the surrounding continents[1,2,3]. The dynamic mechanism underlying Atlantic temperature variability is thought to be similar to that of the El Niño/Southern Oscillation (ENSO) in the equatorial Pacific[4,5], where air–sea coupling leads to a positive feedback between surface winds in the western basin, sea surface temperature in the eastern basin, and equatorial oceanic heat content. Here we use a suite of observational data, climate reanalysis products, and general circulation model simulations to reassess the factors driving the interannual variability. We show that some of the warm events cannot be explained by previously identified equatorial wind stress forcing and ENSO-like dynamics. Instead, these events are driven by a mechanism in which surface wind forcing just north of the equator induces warm ocean temperature anomalies that are subsequently advected toward the equator. We find the surface wind patterns are associated with long-lived subtropical sea surface temperature anomalies and suggest they therefore reflect a link between equatorial and subtropical Atlantic variability.

For decades zonal equatorial wind stress has been recognized as a key component of the Pacific ENSO phenomenon[6,7]. According to ENSO theory a weakening of the trades over the western equatorial Pacific leads to a readjustment of the well-mixed upper ocean layer (typically 50-150m deep). Under this readjustment the mixed layer shoals in the west and deepens in the east, which leads to warming in the eastern equatorial Pacific. Readjustment is achieved through equatorial Rossby and Kelvin waves whose respective propagation speeds lead to a delay between wind stress forcing and ocean response by

several months. More specifically, it takes about 3 months for equatorial Kelvin waves to propagate the warming signal to the eastern equatorial Pacific.

Variability in the equatorial Atlantic is thought to be governed by similar processes as ENSO[4,5,8]. Several studies suggest that westerly surface wind stress anomalies in the western equatorial Atlantic force interannual SST variability in the Atlantic cold tongue region with a delay of 1-2 months[5,9] or 5-6 months[10]. We have re-examined this relation in several datasets for March-April-May (MAM) zonal surface winds in the western/central equatorial Atlantic versus June-July-August (JJA) SST in the eastern equatorial Atlantic (Fig. 1). The rationale for picking these particular seasons lies in the pronounced seasonality of the tropical Atlantic: equatorial wind variability peaks in MAM while SST variability peaks in JJA. In some coupled general circulation models zonal wind and SST are indeed highly correlated at around 0.8[11]. The observational and reanalysis datasets examined here show more scatter with correlations ranging between 0.4 and 0.6, which corresponds to approximately 15-35% explained variance. In other words, 65-85% of equatorial Atlantic variability remains unaccounted for. Moreover, Fig. 1 reveals that some warm events develop despite easterly wind anomalies in the preceding months (upper left quadrant of Fig. 1). The occurrence of such events cannot be explained by ENSO-like dynamics, which should generate cooling under such conditions. We will show that horizontal advection plays a vital role in the evolution of these events, which we will refer to as "non-canonical events" in the following. Events in the upper right quadrant of Fig. 1, on the other hand, are consistent with ENSO-like dynamics, because the warming follows westerly wind anomalies that reduce upwelling in the eastern equatorial Atlantic. These events will be referred to as "canonical events".

Composites of the non-canonical events reveal a very slow evolution of SST anomalies with the whole event lasting for about a year (Fig. 2a; see Methods section for the years used in each composite). This is preceded by easterly wind anomalies that are already present at the beginning of the year and continue until July, with particularly strong anomalies from February to May. After July the easterly wind anomalies subside, which is consistent with the Atlantic Walker cell responding to the maturing warm SST anomaly in the eastern equatorial Atlantic.

In contrast, composites of the canonical events are characterized by rapid development of SST anomalies preceded by westerly wind anomalies (Fig. 2b). The wind anomalies peak in May, while the SST anomalies peak two months later in July.

A joint empirical orthogonal function analysis of NCEP Reanalysis wind and 3-month lagged SST anomalies (Supplementary Fig. 1) yields two important modes. The first mode explains 30% of the coupled variance and resembles the canonical Atlantic Niño, with weakening of the equatorial trades preceding the SST warming. The second mode, on the other hand, features easterly equatorial anomalies followed by SST warming. This pattern, which explains 18% of the coupled variance, is consistent with the non-canonical warm events.

The two types of equatorial warm events differ not only in terms of surface winds but also in terms of northern tropical Atlantic (NTA) SST (see Methods for index definition). Non-canonical events are accompanied by pronounced positive anomalies in the NTA (Fig. 2a), while canonical events are accompanied by weak anomalies of the opposite sign (Fig. 2b).

The horizontal maps of SST composites (Fig. 3) confirm that non-canonical events are marked by widespread SST warming in the northern tropical Atlantic in boreal spring. One season later warming has subsided in the NTA and is most pronounced in the equatorial region instead. Canonical events, on the other hand, do not feature significant equatorial SST anomalies in April (Fig. 3b). Rather, the SST anomalies develop rapidly in June and are clearly confined to the cold tongue and Benguela coastal upwelling region (Supplementary Fig. 2b). Further analysis shows that the NTA warming in non-canonical events is associated with reduced surface latent heat flux and near-surface winds (Supplementary Fig. 2a). This pattern is characteristic of the meridional mode[12,13], which dominates variability in the subtropical Atlantic. Thus the meridional mode appears to be an important element in the developing phase of non-canonical events but its center around 15°N is too far from the equator to allow for a direct oceanic pathway, which indicates an atmospheric link[14,15].

To shed further light on the oceanic dynamics we analyze output from an oceanic general circulation model (GCM) hindcast forced with NCEP reanalysis wind stress and heat fluxes. A heat budget analysis for the upper 50m of the eastern equatorial Atlantic (Fig. 4ab; see Methods) points at a distinct difference between canonical and non-canonical events. While the former are dominated by vertical advection, the latter involve a significant contribution from meridional and zonal advection. Thus, in non-canonical events, warming due to horizontal advection opposes the cooling by vertical advection through June. The zonal component is related to the climatological zonal temperature gradient in the equatorial Atlantic, which features warm temperatures to the east of the cold tongue. Easterly wind anomalies therefore lead to warm advection on the eastern

flank of the cold tongue. The warming by meridional advection is most pronounced below the surface between 20-40m depth, where the ocean temperature anomalies are maximum and the currents flow toward the equator (Supplementary Fig. 3). The cross sections also reveal that while the maximum SST anomalies occur between 10-15°N, the maximum subsurface anomalies are much closer to the equator at around 4°N. This allows the ocean temperature anomalies to have a substantial influence on the equatorial warming even though meridional current speeds are only a few cm/s (Supplementary Fig. 3). The reason for the sub-surface temperature anomalies lies in the negative wind stress curl that drives current convergence and downwelling just north of the equator (Supplementary Fig. 4a). The wind stress curl, in turn, results from the characteristic wind configuration of the meridional mode, in which easterly anomalies on the equator are contrasted by northwesterly anomalies to the north. Previous studies have documented the subsurface impact of the wind stress curl in the northern equatorial Atlantic[15,16].

The observational data record is short and particularly wind measurements are sparse prior to the satellite period. We therefore seek to confirm our results by examining a 1000-year coupled GCM simulation (see Methods) that is able to reproduce some of the observed characteristics of equatorial Atlantic variability, such as the frequency, duration, and preferred occurrence in JJA. As in the observations, the model simulates variations in the wind/SST relation on interdecadal time scales. Composites of the non-canonical and canonical events reveal the same pattern of northern tropical Atlantic warm SST anomalies versus the equatorially confined signal (Figs. 3c and d). These patterns are significant at the 95% confidence level. As in the observations, the northern tropical Atlantic warming is associated with decreased latent heat loss and wind stress induced downwelling

(not shown). Furthermore, the meridional cross sections for non-canonical events show a pattern of warm temperatures and equatorward currents at 30-50m depth, just north of the equator (Supplementary Fig. 5). A heat budget analysis of the eastern equatorial Atlantic suggests that canonical events are dominated by vertical advection while non-canonical events are dominated by meridional and zonal advection (Supplementary Fig. 7), similar to the results from the ocean hindcast. Indeed, the GCM results show an even clearer distinction between the two types of events.

Recent studies[15,16] suggest an alternative pathway for the NTA influence on the equatorial Atlantic. The proposed mechanism involves off-equatorial downwelling Rossby waves generated by the wind stress curl anomalies associated with the meridional mode. Upon reaching the western boundary, these Rossby waves are reflected into downwelling equatorial Kelvin waves and subsequently lead to warming in the eastern equatorial Atlantic. The results presented here (Figs. 4a and Supplementary Fig. 7a), however, indicate that downwelling does not play an important role at the onset of non-canonical events, though it does become important during the mature phase. Furthermore, composited longitude-time sections of upper 100m ocean heat content from the ocean hindcast do not show convincing evidence of Rossby wave reflection (Supplementary Fig. 4a), nor do 3-daily sea-level anomalies for the year 2006 (Supplementary Fig. 8).

The fitted regression lines in Fig. 1 show that in some years SST roughly follow the linear wind/SST relation (dots close to the regression line) while in other years they do not (dots far away from the regression line). The question arises whether this is related to long-term changes in the relative frequency of canonical and non-canonical events. We explore this by calculating a running correlation of MAM zonal surface wind and JJA

SST using a 21-year sliding window (see Methods). This reveals that the strength of the wind/SST relation varies considerably (Fig. 4c), with correlations ranging from 0.1 to 0.7 depending on the period. Both observations and reanalyses roughly agree on a decline of the correlation strength from around 1970 and subsequent recovery in the 1980s, suggesting that this is a robust feature. Since it is difficult to get a reliable estimate of the correlation strength from a short time series, we substantiate our results by fitting a simple linear relation to the data and calculating the residuals (see Methods). This additional measure of the wind/SST relation (denoted by the blue line in Figs. 4c-f) agrees quite well with the running correlation, particularly in the ICOADS and NCEP reanalysis data.

While our results suggest a link between the meridional mode and non-canonical equatorial warming, we note that the two are separate phenomena. The meridional mode is centered in the subtropics (around 15°), driven by latent heat flux anomalies, damped by oceanic horizontal advection, and most active during boreal spring. The non-canonical Atlantic Niño, on the other hand, is centered on the equator, driven by horizontal advection, damped by latent heat flux, and peaks in boreal summer. Moreover, warm NTA anomalies do not always result in equatorial warm events. In fact, composites of canonical Atlantic Niñas (Supplementary Fig. 4c) demonstrate that NTA warming can be followed by cold events on the equator. Whether a positive meridional mode is followed by a non-canonical warm event depends on the subsurface temperature anomalies it induces just north of the equator, and likely several other factors such as preconditioning of the equatorial Atlantic and influences from the equatorial Pacific.

Methods

Observations. We use monthly mean ship observations of SST and near-surface winds from the International Comprehensive Ocean-Atmosphere Dataset[17] (ICOADS; version 2.5). The period 1960-2010 was analyzed and the climatological seasonal cycle based on this period was subtracted to obtain monthly anomalies.

Reanalyses. The National Center for Environmental Prediction (NCEP) reanalysis[18] for the period 1948-2010 and the European Centre for Medium-range Weather Forecast reanalysis[19] for the period 1958-2001 (ERA-40) were used. Monthly anomalies were calculated based on the climatology for the entire time series.

Models. The coupled GCM in this study is the Commonwealth Scientific and Industrial Research Organisation (CSIRO), version Mk 3.5. A 1000-year integration with pre-industrial greenhouse gas forcing performed for the Coupled Model Intercomparison Project (CMIP) round 3 was downloaded from the CMIP3 archive (http://www-pcmdi.llnl.gov/ipcc/about_ipcc.php). The simulated tropical Atlantic climate suffers some of the typical GCM biases[20] including a weak equatorial cold tongue in JJA. Compared to other CMIP3 models, however, these biases are moderate. Most importantly, interannual variability is reasonably well reproduced.

The ocean hindcast model is the OGCM for the Earth Simulator (OFES; see refs. 22 and 23 for details), with a resolution of 0.1 in the horizontal and 54 vertical levels. The model is run from 1950-present and forced with surface fluxes of heat, momentum and

freshwater based on the NCEP Reanalysis. OFES reproduces fairly accurately the tropical Atlantic SST of the NCEP reanalysis. There are, however, years with considerable differences and this influences the categorization of events to some extent (see **Categorization of events** below).

Index regions. The equatorial Atlantic cold tongue index (ACT1) was calculated as the area averaged SST for the region (15-5°W, 3°S-3°N). The western equatorial Atlantic surface wind index (WEA) was calculated as the average of surface winds over (40-10°W, 2°S-2°N). Finally, the NTA SST index is defined as SST averaged over (40-10°W, 10-20°N).

Estimation of the strength of the wind/SST relation. The strength of the wind/SST relation was derived by taking the MAM average of WEA zonal surface wind for each year and correlating it with the corresponding JJA average of ACT1 SST. A 21-year running window was applied to obtain the running correlation. The values are somewhat sensitive to the spatial extent of the averaging areas for wind and SST but the qualitative features, including the decline of correlation strength in the 1970s, are robust.

As a second measure of the wind/SST relation we assumed that a perfect correlation between (standardized) MAM zonal surface wind and JJA SST would be represented by a line with slope 1 and offset 0, i.e. 1 standard deviation in zonal surface winds leads to 1 standard deviation in SSTs. We then calculate the absolute difference between the actual and "predicted" SST and use a 21-year running window to calculate a running average.

Categorization of events. Canonical and non-canonical events are categorized based on the wind/SST relationship under the assumption that the equatorial Atlantic dynamics should be governed by ENSO-like dynamics. In that case one would expect warm SST in the east to be preceded by westerly wind anomalies in the western/central equatorial Atlantic. We define positive wind events as instances when the MAM zonal surface wind anomaly in the WEA area exceeds 0.5 (falls below -0.5) standard deviations. SST events are defined analogously using JJA SST anomalies in the ACT1 area. A warm SST event is categorized as a canonical (non-canonical) event when it is preceded by a positive (negative) surface wind anomaly. Cold SST events are categorized in the same way. In terms of the scatter plots in Figure 1a, canonical events lie in the upper right and lower left while non-canonical events lie in the upper left and lower right quadrants. Based on NCEP reanalysis, non-canonical (canonical) warm events occur in years 1951, 1979, 1987, 1998, 2006, and 2010 (1949, 1963, 1968, 1974, 1991, and 2008). For the OFES hindcast, the selected years are 1979, 1987, 1998, and 2006 (1957, 1960, 1963, 1968, 1988, 1991, 1996, and 2008). Note that 1984, which was a pronounced Atlantic Niño, is not included because winds were near neutral and thus neither category applied.

Global warming trend. The tropical Atlantic has been subject to long-term temperature and surface wind changes over the last several decades (Tokinaga and Xie, 2011). Since such trends in the data influence the correlation analysis, the linear trend has been removed from all time series.

Heat budget analysis. See Supplementary Material.

Correspondence statement

Correspondence and requests should be addressed to Ingo Richter (richter@jamstec.go.jp).

Acknowledgments

The authors would like to thank Shang-Ping Xie, Axel Timmermann, and Fei-Fei Jin for their comments on this work. OFES integrations were carried out at the Earth Simulator Center, Yokohama, Japan. We acknowledge the modeling groups, the Program for Climate Model Diagnosis and Intercomparison (PCMDI) and the WCRP's Working Group on Coupled Modelling (WGCM) for their roles in making available the WCRP CMIP3 multi-model data set. Support of this data set is provided by the Office of Science, US Department of Energy.

Author Contributions

Ingo Richter conceived the central idea, carried out the analysis, and wrote the paper. Hideharu Sasaki performed the OFES hindcast integrations. All authors provided guidance for the analysis and commented on the manuscript.

References

1. Carton, J. A. & Huang, B. Warm events in the tropical Atlantic. *J. Phys. Oceanogr.* **24,** 888–903 (1994)

2. Carton, J. A., Cao, X., Giese, B. S. & da Silva A. M. Decadal and interannual SST variability in the tropical Atlantic Ocean. *J. Phys. Oceanogr.* **26,** 1165–1175 (1996)

3. Folland, C. K., Colman A. W., Powell, D. P. & Davey, M. K. Predictability of northeast Brazil rainfall and real-time forecast skill, 1987–98. *J. Clim.* **14,** 1937–1958 (2001)

4. Zebiak, S. E. Air–sea interaction in the equatorial Atlantic region. *J. Clim.* **6,** 1567–1586 (1993)

5. Keenlyside, N. S. & Latif, M. Understanding equatorial Atlantic interannual variability. *J. Clim.* **20,** 131-142 (2007)

6. Wyrtki, K. El Niño—the dynamic response of the equatorial Pacific ocean to atmospheric forcing. J. Phys. Oceanogr. **5,** 572-584 (1975)

7. Rasmusson, E. M. & Carpenter, T. H. Variations in Tropical Sea Surface Temperature and Surface Wind Fields Associated with the Southern Oscillation/El Niño. *Mon. Wea. Rev.* **110**, 354–384 (1982)

8. Philander, S. G. H. Unusual conditions in the tropical Atlantic Ocean in 1984. *Nature* **322,** 236–238 (1986)

9. Servain, J., Picaut, J. & Merle, J. Evidence of remote forcing in the equatorial Atlantic Ocean. *J. Phys. Oceanogr.* **12,** 457–463 (1982)

10. Vauclair, F. & du Penhoat, Y. Interannual variability of the upper layer of the tropical Atlantic from in situ data between 1979 and 1999. *Clim. Dynam.* **17,** 527–546 (2001)

11. Richter, I., Xie, S.-P., Wittenberg, A. T. & Masumoto, Y. Tropical Atlantic biases and their relation to surface wind stress and terrestrial precipitation. *Clim. Dynam.* **38**, 985-1001, doi: 10.1007/s00382-011-1038-9 (2012)

12. Servain, J. Simple climate indices for the tropical Atlantic Ocean and some applications. *J. Geophys. Res.* **96,** 15,137–15,146 (1991)

13. Nobre, P. & Shukla, J. Variations of Sea Surface Temperature, Wind Stress, and Rainfall over the Tropical Atlantic and South America. *J. Clim.* **9,** 2464-2479 (1996)

14. Servain, J., Wainer, I., McCreary, J. P. & Dessier, A. Relationship between the equatorial and meridional modes of climate variability in the tropical Atlantic. *Geophys. Res. Lett.* **26,** 458–488 (1999)

15. Foltz, G. R. & McPhaden, M. J. Interaction between the Atlantic meridional and Niño modes. *Geophys. Res. Lett.* **37**, L18,604, doi:10.1029/2010GL044,001 (2010)

16. Luebbecke, J. & McPhaden, M. J. On the inconsistent relationship between Pacific and Atlantic Niños, *J. Clim.* **25,** 4294-4303 (2012)

17. Woodruff, S. D. *et al*. ICOADS Release 2.5: Extensions and enhancements to the surface marine meteorological archive. *Int. J. Climatol.* **31,** 951-967 (2011).

18. Kalnay, E. *et al.* The NCEP/NCAR 40-Year Reanalysis Project. *Bull. Amer. Meteor. Soc.* **77,** 437–471 (1996)

19. Uppala, S. M. *et al.* 2005: The ERA-40 Re-Analysis. *Quart. J. Roy. Meteor. Soc.* **131**, 2961–3012 (2005)

20. Richter, I. & Xie, S.-P. On the origin of equatorial Atlantic biases in coupled general circulation models, *Clim. Dyn.* **31**, 587–598, doi:10.1007/s00382-008-0364-z (2008)

21. Sasaki, H. *et al.* An eddy-resolving hindcast simulation of the quasi-global ocean from 1950-2003 on the Earth Simulator. In *High Resolution Numerical Modeling of the Atmosphere and Ocean*, K. Hamilton and W. Ohfuchi (eds.), chapter 10, pp. 157-185, Springer, New York (2008)

22. Masumoto, Y. Sharing the results of a high-resolution ocean general circulation model under a multi-discipline framework: a review of OFES activities. *Ocean Dyn.* **60,** 633-652 (2010)

23. Tokinaga, H. & Xie, S.-P. Weakening of the equatorial Atlantic cold tongue over the past six decades. *Nature Geosci.* **4**, 222-226, doi:10.1038/ngeo1078 (2011)

Figure Captions

Figure 1 | Correlation between equatorial boreal spring surface winds and cold tongue summer SST for 4 datasets. Scatter plot of MAM WEA index (zonal surface wind anomaly averaged over 40°-10°W, 2°S-2°N) versus JJA ACT1 index (SST anomaly averaged over 15°-5°W, 3°S-3°N). Every dot corresponds to one year. Values have been normalized by their respective standard deviation and the dashed lines mark -0.5 and +0.5 on the x and y-axes. The datasets are (from upper left to lower right) ICOADS observations, ERA-40 and NCEP reanalyses, and the CSIRO Mk 3.5 coupled GCM simulation.

Figure 2 | Composite evolution of equatorial Atlantic warm events in the NCEP reanalysis. a, Evolution of non-canonical events. Western equatorial Atlantic zonal surface wind anomaly (green line), eastern equatorial Atlantic SST anomaly (blue line), and northern tropical Atlantic SST anomaly (orange line). Evolution is shown from January of the peak year to the following January. Indices are normalized by their standard deviation. Dots denote values significant at the 90% confidence level. **b**, Evolution of canonical events.

Figure 3 | Composite maps showing the evolution of non-canonical and warm canonical events in April and July. a, **b**, SST anomalies (shading; in Kelvin) in the NCEP reanalysis for non-canonical (a) and canonical (b) events. Values significant at the 90% confidence level are shaded. **c**, **d**, SST (shading; in Kelvin) anomalies in the CSIRO Mk 3.5 1000-year simulation for non-canonical (c) and canonical (d) events. Values signifi-

cant at the 95% confidence level are shaded. Note that March and June are shown for the canonical events in CSIRO Mk 3.5 because these peak earlier in the year.

Figure 4 | Heat budget terms in the eastern equatorial Atlantic for the OFES hindcast, and running correlation of wind and SST anomalies in 4 datasets. a, b, Net surface heat flux (red), vertical advection (brown), meridional advection (orange), zonal advection (blue), and temperature tendency (green) in the eastern equatorial Atlantic (ACT1 region) for OFES. Dots denote values significant at the 90% confidence level. The panels show composites for non-canonical events (a) and canonical events (b). **c, d, e, and f**, Running correlation (green line) of the MAM WEA and JJA ACT1 indices, and averaged absolute distance (blue line) of the points in Fig. 1 from a 1-to-1 regression line. Both lines are calculated using a 21-year sliding window. The datasets shown are ICOADS (c), ERA-40 (d), NCEP Reanalysis (e), and the CSIRO Mk 3.5 coupled GCM (f).

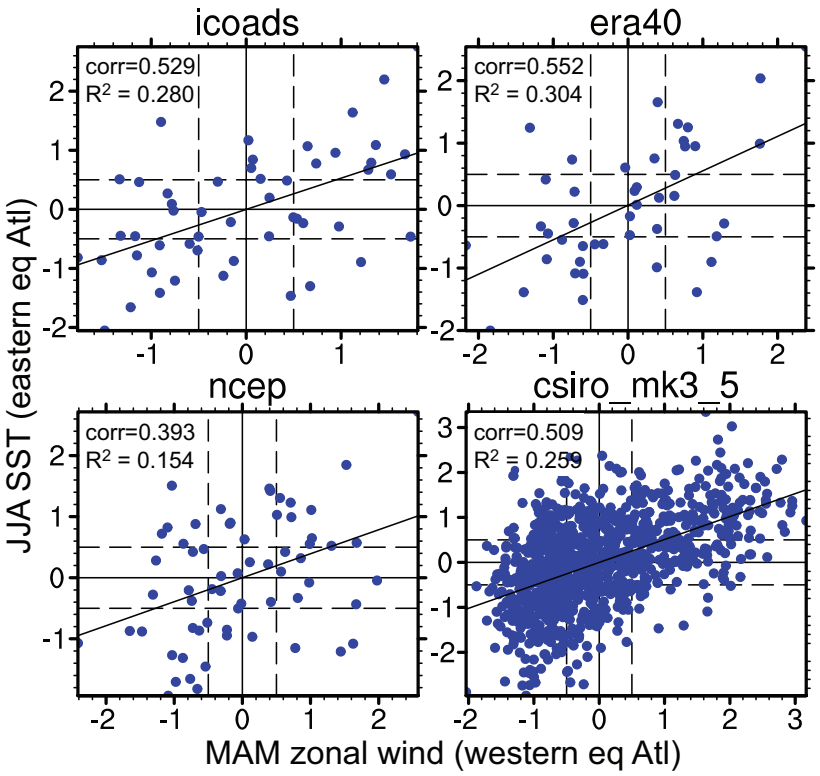

Figure 1 | Correlation between equatorial boreal spring surface winds and cold tongue summer SST for 4 datasets. Scatter plot of MAM WEA index (zonal surface wind anomaly averaged over 40°-10°W, 2°S-2°N) versus JJA ACT1 index (SST anomaly averaged over 15°-5°W, 3°S-3°N). Every dot corresponds to one year. Values have been normalized by their respective standard deviation and the dashed lines mark -0.5 and +0.5 on the x and y-axes. The datasets are (from upper left to lower right) ICOADS observations, ERA-40 and NCEP reanalyses, and the CSIRO Mk 3.5 coupled GCM simulation.

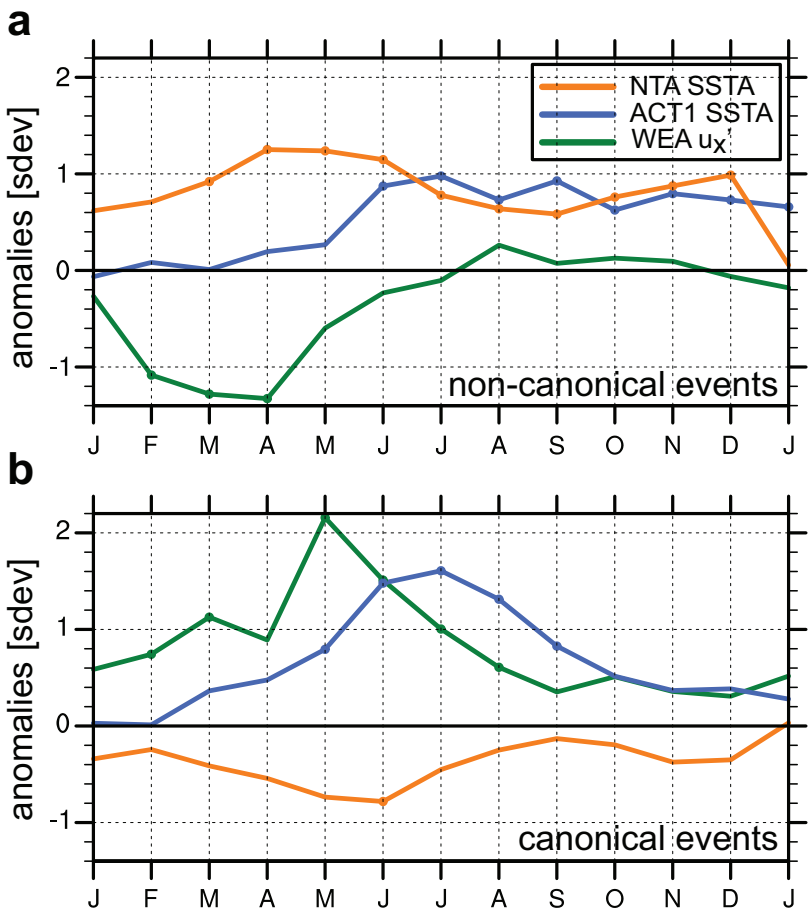

Figure 2 | Composite evolution of equatorial Atlantic warm events in the NCEP reanalysis. a, Evolution of non-canonical events. Western equatorial Atlantic zonal surface wind anomaly (green line), eastern equatorial Atlantic SST anomaly (blue line), and northern tropical Atlantic SST anomaly (orange line). Evolution is shown from January of the peak year to the following January. Indices are normalized by their standard deviation. Dots denote values significant at the 90% confidence level. **b**, Evolution of canonical events.

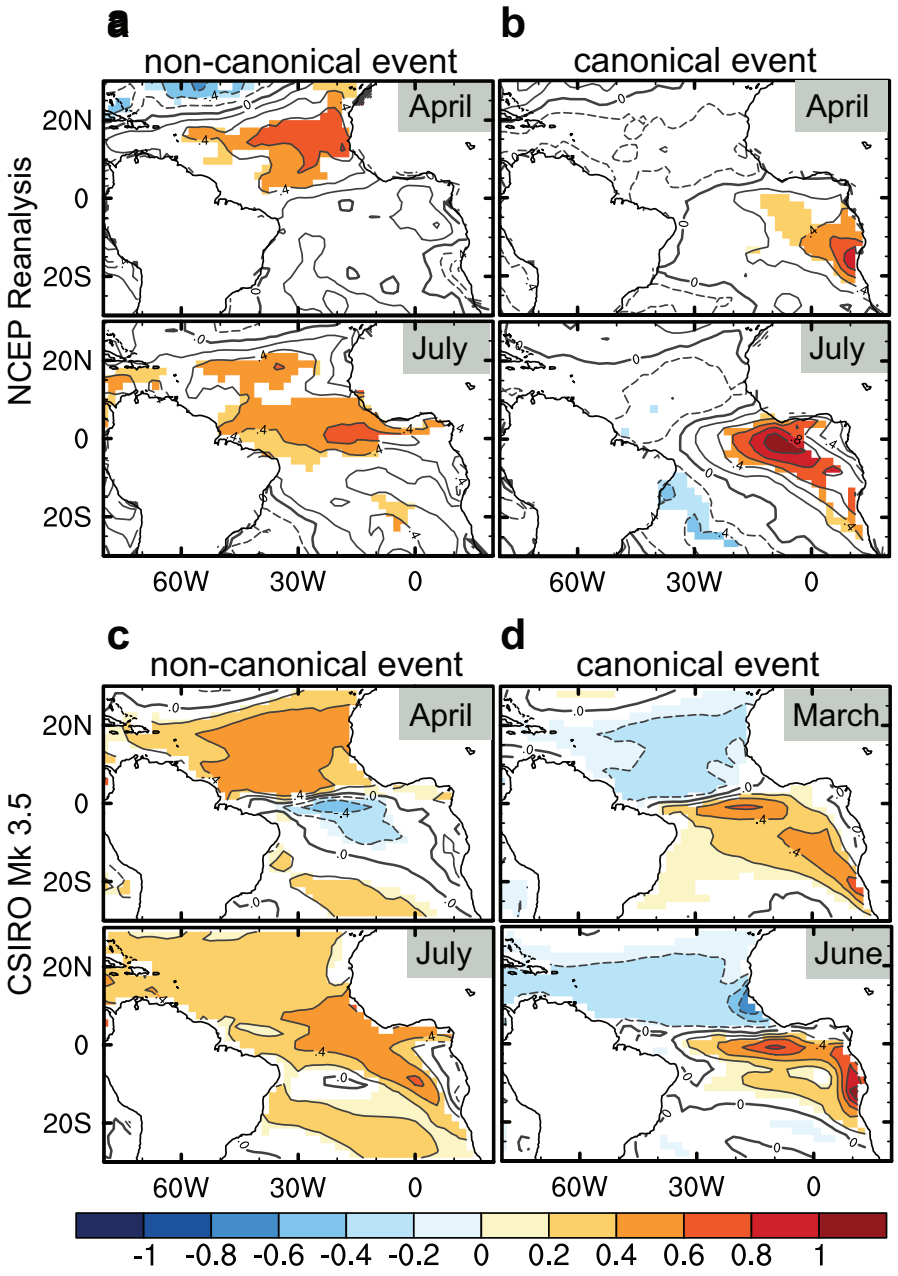

Figure 3 | Composite maps showing the evolution of non-canonical and warm canonical events in April and July. a, **b**, SST anomalies (shading; in Kelvin) in the NCEP reanalysis for non-canonical (a) and canonical (b) events. Values significant at the 90% confidence level are shaded. **c**, **d**, SST (shading; in Kelvin) anomalies in the CSIRO Mk 3.5 1000-year simulation for non-canonical (c) and canonical (d) events. Values significant at the 95% confidence level are shaded. Note that March and June are shown for the canonical events in CSIRO Mk 3.5 because these peak earlier in the year.

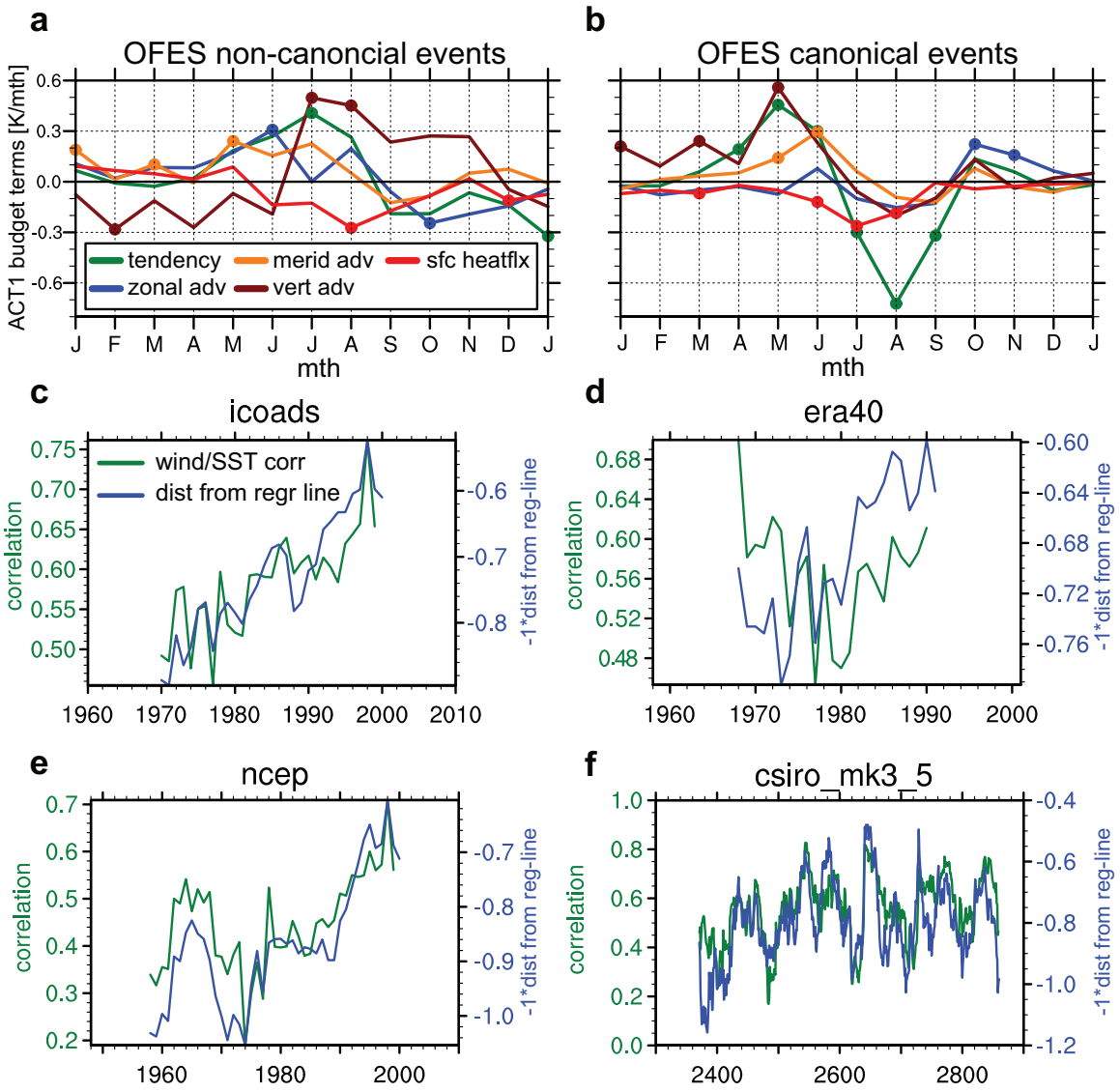

Figure 4 | Heat budget terms in the eastern equatorial Atlantic for the OFES hindcast, and running correlation of wind and SST anomalies in 4 datasets. a, b, Net surface heat flux (red), vertical advection (brown), meridional advection (orange), zonal advection (blue), and temperature tendency (green) in the eastern equatorial Atlantic (ACT1 region) for OFES. Dots denote values significant at the 90% confidence level. The panels show composites for non-canonical events (a) and canonical events (b). **c, d, e, and f**, Running correlation (green line) of the MAM WEA and JJA ACT1 indices, and averaged absolute distance (blue line) of the points in Fig. 1 from a 1-to-1 regression line. Both lines are calculated using a 21-year sliding window. The datasets shown are ICOADS (c), ERA-40 (d), NCEP Reanalysis (e), and the CSIRO Mk 3.5 coupled GCM (f).